OPTOELECTRONICS AND ADVANCED MATERIALS – RAPID COMMUNICATIONS Vol. 12, No. 9-10, September-October 2018, p. 584 - 587

Investigation of the optical properties on $Ge_2Sb_2Te_5$/Si superlattice-like thin films

L. ZHENG[a,*], Y. HU[a], J. XU[b], H. ZOU[a], X. ZHU[a], L. ZHAI[a], B. LIU[a], J. XUE[a], Y. SUI[a], M. PEI[a]
[a]*School of Mathematics and Physics, Jiangsu University of Technology, Changzhou 213001, China*
[b]*Key Laboratory of Radio Frequency and Micro-Nano Electronics of Jiangsu Province, Nanjing 210023, Jiangsu, China*

We employ the spectroscopic ellipsometry technique to study the optical properties in $Ge_2Sb_2Te_5$/Si superlattice-like thin films because of the potential use in optical storage. In the reflectivity measurements on the amorphous state, it is found that the reflection spectra could be substantially modified by changing the film thickness, the polarized direction of the light and the incident angle θ, respectively. It is believed that more Ge atoms in ultrathin films are tetrahedrally coordinated instead of the defective octahedral-like sites and brings about the evolution of the optical reflectivity. The isotropic resonant bonding environment in the crystallization state is also observed by the reflection spectra.

(Received June 22, 2017; accepted October 10, 2018)

Keywords: Superlattice-like thin films, $Ge_2Sb_2Te_5$, Reflection spectra

1. Introduction

$Ge_2Sb_2Te_5$ (GST) is a popular reversible phase-change compound, as it widely used in optical storage (DVDs) and also in electrical phase-change memory devices [1]. The basic concept of the reversible phase-change memory is based on the rapid reversible phase change between amorphous and crystalline states induced by Joule heating [2]. There is a huge deference in the resistivity between the amorphous state and the crystalline state for GST, this difference is attributed to a significant change in bonding between the two phases [3-4]. The amorphous phase is that expected of a covalent semiconductor, Ge atoms generally prefer to be sp^3 hybridized and tetrahedrally coordinated when forming covalent bonds with its neighbors [5]. In spite of this, resonant bonds are partially preserved in the amorphous phase, as is evidenced by the existence of so-called defective octahedral sites [6]. In the crystalline state, crystalline phase is strongly enhanced by resonant bonding effect, each atom is bonded to its first nearest neighbors [7]. Covalent (tetrahedral and/or pyramidal) configurations characteristic of the amorphous phase and resonant configurations characteristic of the crystalline phase [8].

It has been demonstrated that when the thickness of phase change film decreases, size effects will play an important role in the crystallization temperature, crystallization speed and other parameters of the material [9]. Yu et al. has indicated the drastic effect of film thickness on the local order of Ge sites in amorphous GeTe ultrathin film, more Ge atoms in ultrathin films are tetrahedrally coordinated instead of the defective octahedral-like sites [10]. Although such macroscopic properties of phase change have been widely investigated, the microscopic structural evolution of the amorphous films is still not clear. Because of the differences between the tetrahedral and defective octahedral sites were rather small and hard to be detected in the amorphous state [11]. Generally, the reflection spectra in the amorphous phase could demonstrate pronounced differences between the tetrahedral and defective octahedral-like sites [8]. Because the optical reflectivity is determined by the combination of the refractive index and extinction coefficient [12].

In this report, we employ the spectroscopic ellipsometry technique to study the optical properties in GST/Si superlattice-like (SLL) thin films in both amorphous and crystallization states. SLL GST materials have been widely investigated because it can fulfill the requirement for ideal phase-change materials with high crystallization speed and thermal stability [13]. In the SLL films, a high interface-to-volume ratio can induce larger structure modification because of the surface reactivity and chemical affinity [14]. Stress effect in the interface will be exacerbated with the decreasing layer thickness and result in a considerable interfacial atomic arrangement [15-17]. As the result, the optical properties in the SLL films will be changed. It is very important to investigate the optical properties because of the potential application in optical storage. In the reflection spectra measurements, the optical properties and the evolution of atomic bonding environment in these samples are discussed.

2. Experimental

The $[GST(10nm)/Si(10nm)]_{10}$, $[GST(8nm)/Si(8nm)]_{10}$ and $GST(6nm)/Si(6nm)]_{10}$ SLL thin films were sputtered as previous report [17]. Briefly, the GST/Si SLL thin films were sputtered on a SiO_2/Si(1 0 0) wafer by alternately sputtering GST and Si targets using controlled deposition cycles at room temperature. The background pressure was below 3×10^{-5} Pa and the sputtering pressure was 0.5 Pa. Both the sputtering power of GST and Si target were set to 20 W. The total thickness of the GST/Si SLL films was controlled by deposition time. The as-deposited films surface was GST and the GST were in the amorphous phase. The amorphous phase and the crystalline state (after annealing at 200 °C in air for 5 min) were examined by X-ray diffraction, using Rigaku Dmax-rB diffractometer. Optical constant of the prepared SLL films was obtained from the analysis of spectroscopic ellipsometry data measured using an ellipsometer with an automatic rotating analyzer (VASE, J. A. Woollam Co., Inc.), in the wavelength range 600nm-1650nm. All measurements were carried out at room temperature.

3. Results and discussions

In order to intuitively understand the chemical bonding origin of optical contrast of the three samples, in as-deposited state and the crystalline state, spectroscopic ellipsometry data were determined. Fig. 1 illustrates the schematic view of the experimental setup in the optical reflectivity measurement. The s-polarized and p-polarized lights were performed in the study. Incident angle θ dependence of the reflection strength were also carried out to estimate the chemical bonding evolution. Fig. 2 illustrates the optical spectra for amorphous [GST (10nm)/Si $(10nm)]_{10}$, [GST (8nm)/Si $(8nm)]_{10}$ and GST (6nm)/Si $(6nm)]_{10}$ with polarized excitations. In fact, the incident angles θ, are 45º, 50º, 55º, 60º and 65º to the sample normal are selected in the experiment. However, too many curves in the figure is hard to distinguish it clearly for readers. As the result, spectra from three angles are selected in the figure and does not affect the data analysis.

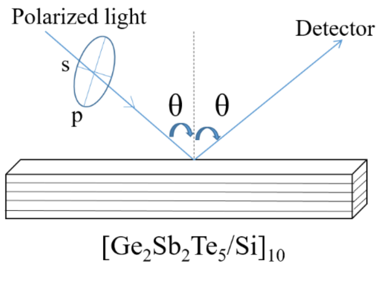

Fig. 1. Schematic of the polarized light and incident angle θ dependence of the reflection intensity measurements. The s and p indicate the s-polarized and p-polarized light, respectively

Those visible characters in the spectra should be taken into account: 1. film thickness dependence of the reflection spectra; 2. the different reflection spectra for s-polarized and p-polarized excitations; 3. the evolution on reflection spectra the variation of incident angle θ. Those characters enable us to give an unambiguous interpretation for optical properties and the bonding environment in the amorphous state.

In Fig. 2, the reflection spectra show a single absorption peak (the low reflectivity region, marked with vertical lines). The reflection spectra are changed substantially with adjusting the layer thickness. Table 1 illustrates the absorption peak positions in the reflection spectra for the three samples. This peak is found gradually moved to higher energy with decreasing the layer thickness. Generally, this remarkable change belonging to the appreciable structural rearrangement [12]. In the SLL structure, atomic arrangement at the interface is important because of the relatively high coordination number of Ge element, which can strengthen of the covalent bonds with neighboring atoms [8]. In the amorphous GST, Ge atoms can occupy both the fourfold and tetrahedral sites [7]. More Ge atoms in ultrathin films tend to tetrahedral coordinated rather than the octahedral one, while the latter is more similar to its local structure in crystalline phase [10]. The layer thickness dependence of the shift in the absorption peak positions should be related with the Ge bonding environment change.

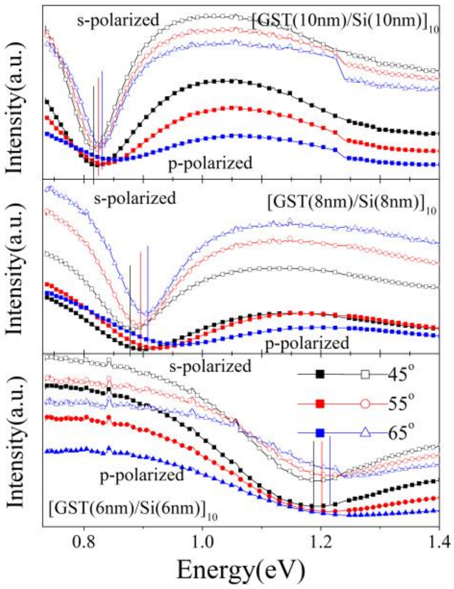

Fig. 2. The reflection spectra of amorphous [GST (10nm)/Si $(10nm)]_{10}$, [GST (8nm)/Si $(8nm)]_{10}$ and GST (6nm)/Si $(6nm)]_{10}$ with the s-polarized (hollow symbol) and p-polarized (solid symbol) excitations. The incident angles θ, are 45º, 55º and 65º to the sample normal are selected in the experiment

The reflection spectra for s-polarized and p-polarized excitations are quite different as can be seen in Fig. 2. It is believed that weaker Ge-Te bonds will be broken during the displacement of Ge atoms in the structure [18]. The displacement of Ge atoms could be enhanced when exciting with p-polarized excitation, as the p-polarized excitation would generate stronger anisotropic photo-excited carrier distribution rather than the s-polarized excitation [19]. This in turn brings about the evolution of optical reflectivity. Very small difference of the peak position between s-polarized and p-polarized excitations in GST (6nm)/Si (6nm)]$_{10}$ could be observed, as seen in Table 1. The anisotropic photo-excited carrier distribution is easier to be generated in the amorphous [GST (6nm)/Si (6nm)]$_{10}$ because of the enhanced covalent bonding environment [20].

The evolution of reflection spectra with various incident angles, should be related with the electronic polarizability and the chemical bonds. In the amorphous GST, majority of Ge atoms are covalent bonded with other atoms in tetrahedral or octahedral environment [21,22]. In the isotropic resonant bonding environment of the crystalline state, each atom is bonded to its first nearest neighbors, the absorption properties are not sensitive to the excitation direction of the lights. It is understandable that the θ dependence of the position are negligible small when exciting with s-polarized lights in amorphous [GST (10nm)/Si (10nm)]$_{10}$ (see table 2). And the stronger peak shift in amorphous [GST (8nm)/Si (8nm)]$_{10}$ and GST (6nm)/Si (6nm)]$_{10}$ could be observed. Still, this behavior is stronger when exciting with p-polarized excitations.

Table 1. The absorption peak position in the reflection spectra for amorphous [GST (10nm)/Si (10nm)]$_{10}$, [GST (8nm)/Si (8nm)]$_{10}$ and GST (6nm)/Si (6nm)]$_{10}$. The s and p indicate the s-polarized and p-polarized excitations, respectively. Δ_{sp} indicate the difference of peak position between s- and p-polarized excitations

	45° (eV)			55° (eV)			65° (eV)		
	s	p	Δ_{sp}	s	p	Δ_{sp}	s	p	Δ_{sp}
[GST (10nm)/Si (10nm)]$_{10}$	0.816	0.821	0.005	0.822	0.834	0.012	0.829	0.856	0.027
[GST (8nm)/Si (8nm)]$_{10}$	0.882	0.901	0.019	0.892	0.922	0.03	0.906	0.960	0.054
GST (6nm)/Si (6nm)]$_{10}$	1.194	1.191	0.003	1.214	1.213	0.001	1.241	1.240	0.001

Table 2. The evolution of the absorption peak position from 55° to 45° and 65° to 55° in the polarized reflection spectra for amorphous [GST (10nm)/Si (10nm)]$_{10}$, [GST (8nm)/Si (8nm)]$_{10}$ and GST (6nm)/Si (6nm)]$_{10}$

	55°-45° (eV)		65°-55° (eV)	
	s	p	s	p
[GST (10nm)/Si (10nm)]$_{10}$	0.006	0.013	0.007	0.022
[GST (8nm)/Si (8nm)]$_{10}$	0.01	0.021	0.014	0.038
GST (6nm)/Si (6nm)]$_{10}$	0.02	0.022	0.027	0.027

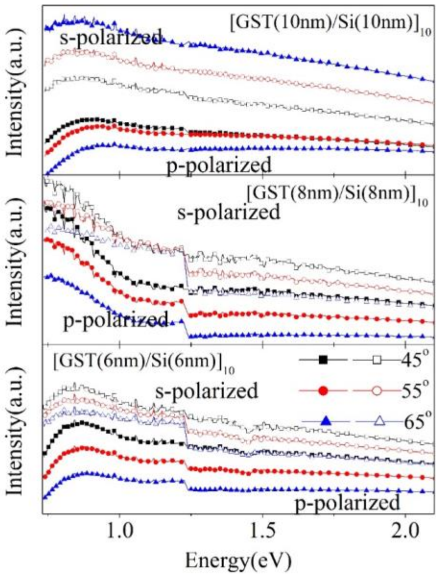

Fig. 3. The reflection spectra the crystalline [GST (10nm)/Si (10nm)]$_{10}$, [GST (8nm)/Si (8nm)]$_{10}$ and GST (6nm)/Si (6nm)]$_{10}$ with the s-polarized (hollow symbol) and p-polarized (solid symbol) excitations. The three crystalline samples were annealed at 200 °C for 5 min

Because of the phase change, large differences could be expected in the reflection spectra between amorphous and crystalline state. The reflection spectra of crystalline [GST (10nm)/Si (10nm)]$_{10}$, [GST (8nm)/Si (8nm)]$_{10}$ and GST (6nm)/Si (6nm)]$_{10}$ are illustrated in the Fig. 3. The distinct reflection characters between the amorphous and the crystalline state can be observed, which has been used for the rewritable optical media DVDs [23]. Because of the large difference of the thermal expansion coefficient between GST and Si, considerably large stress will be generated and applied to the crystalline GST. The thicker the GST layer thickness, the stronger the influence to the GST. There is no distinct difference of the reflection spectra in the three samples, as can be seen in Fig. 3. Resonant interaction is believed dominated in crystalline GST. It could be inferred that the Ge isotropic resonant bonding nature plays an important on the reflection properties, rather than the stress effect.

4. Conclusions

The optical properties on $Ge_2Sb_2Te_5$/Si SLL films are investigated by polarized excitations. We found the reflection spectra in the amorphous phase show pronounced differences in the three samples. Those behaviors are believed to be related with the changing of Ge bonding environment, this in turn brings about the evolution of optical reflectivity. The $Ge_2Sb_2Te_5$/Si SLL films may have the potential for optical storage applications.

Acknowledgments

This work was supported by the Natural Science Foundation of Jiangsu Province [BK20151172]; the University Natural Science Foundation of Jiangsu Province [16KJB140004], Changzhou Science and Technology Bureau (CJ20160028 and CJ20159049) and sponsored by Qing Lan Project.

References

[1] W. Tsai, C. Wang, C. Chen, P. C. Wu, Y. Chen, T. Chen, P. R. Wu, J. Chen, D. P. Tsai, Scientific Reports **7**, 42076 (2017).

[2] T. Guo, S. Song, L. Li, X. Ji, C. Li, C. Xu, L. Shen, Y. Xue, B. Liu, Z. Song, M. Qi, S. Feng, Scripta Materialia **129**, 56 (2017).

[3] Y. G. Choi, S. Y. Shin, R. Golovchak, B. Cheong, H. Jain, Journal of Alloys and Compounds **686**, 273 (2016).

[4] J. Park, S. H. Eom, H. Lee, J. L. F. Da Silva, Y. Kang, T. Lee, Y. H. Khang, Phys. Rev. B **80**, 115209 (2009).

[5] K. V. Mitrofanov, A. V. Kolobov, P. Fons, X. Wang, J. Tominaga, Y. Tamenori, T. Uruga, N. Ciocchini, D. Ielmini, J. Appl. Phys. **115**, 173501 (2014).

[6] J. Hegedus, S. Elliott, Nat. Mater. **7**, 399 (2008).

[7] A. V. Kolobov, M. Krbal, P. Fons, J. Tominaga, T. Uruga, Nat. Chem. **3**, 311 (2011).

[8] K. Shportko, S. Kremers, M. Woda, D. Lencer, J. Robertson, M. Wuttig, Nat. Mater. **7**, 653 (2008).

[9] X. Zhou, J. Kalikka, X. Ji, L. Wu, Z. Song, R. E. Simpson, Adv. Mater. **28**, 3007 (2016).

[10] N. N. Yu, H. Tong, J. Zhou, A. A. Elbashir, X. S. Miao, Appl. Phys. Lett. **103**, 061910 (2013).

[11] Y. G. Choi, A. Kovalskiy, B. K. Cheong, H. Jain, Chemical Physics Letters **534**, 58 (2012).

[12] J. W. Park, M. Song, S. Yoon, H. Lim, D. S. Jeong, B. Cheong, H. Lee, Phys. Status Solidi A **210**, 267 (2013).

[13] L. Zheng, X. Zhu, L. Zhai, Y. Hu, H. Zou, B. Liu, M. Pei, Z. Song, Eur. Phys. J. Appl. Phys. **77**, 30102 (2017).

[14] N. Ohshima, J. Appl. Phys. **83**, 5244 (1998).

[15] R. E. Simpson, M. Krbal, P. Fons, A. V. Kolobov, J. Tominaga, T. Uruga, H. Tanida, Nano Lett. 10, **414** (2010).

[16] J. Fu, X. Shen, Y. Xu, G. Wang, Q. Nie, C. Lin, S. Dai, T. Xu, R. Wang, Mater. Lett. **88**, 148 (2012).

[17] L. Zheng, X. Gu, L. Ma, X. Wu, X. Zhu, Y. Sui, J. Appl. Phys. **119**, 044901 (2016).

[18] K. Makino, J. Tominaga, A. V. Kolobov, P. Fons, M. Hase, Appl. Phys. Lett. **101**, 232101 (2012).

[19] T. Pfeifer, W. Kutt, H. Kurz, R. Scholz, Phys. Rev. Lett. **69**, 3248 (1992).

[20] C. W. Chiu, Y. C. Huang, F. L. Shyu, M. F. Lin, Opt. Lett. **36**, 3136 (2011).

[21] D. A. Baker, M. A. Paesler, G. Lucovsky, S. C. Agarwal, P. C. Taylor, Phys. Rev. Lett. **96**, 255501 (2006).

[22] G. C. Sosso, S. Caravati, R. Mazzarello, M. Bernasconi, Phys. Rev. B **83**, 134201 (2011).

[23] A. V. Kolobov, P. Fons, A. I. Frenkel, A. L. Ankudinov, J. Tominaga, T. Uruga, Nature Materials **3**, 703 (2004).

---

[*] Corresponding author: zhengphy@163.com